Challenges in the Additive Manufacture of Single and Multi-Core Optical Fibres

Challenges in the Additive Manufacture of Single and Multi-Core Optical Fibres

J. Canning[1,2], Y. Chu[2,3], Y. Luo[2], G.D. Peng[2], J. Zhang[3]
[1] Laseire Consulting Pty Ltd Sydney, NSW 2031, Australia & School of Chemistry University of Sydney, NSW 2006 Australia
[2] National Fibre Facility, School of Electrical & Telecommunications Engineering, University of NSW, (UNSW), Sydney, NSW 2052, Australia
[3] Key Laboratory of In-fiber Integrated Optics of Ministry of Education, College of Physics and Optoelectronic Engineering, Harbin Engineering University, Harbin 150001, China
Email – canning.john@outlook.com

Abstract. Single and multi-core preforms doped with Bi and Er are fabricated using additive manufacture and drawing into optical fibre. We observe an increasing trend towards shape distortion with increasing number of cores. This is explained by noting that the composite effective softening point falls as the number of doped cores rises. The use of a silica cladding tube elevates the drawing temperature unnecessarily.

1. Introduction

Additive manufacture of application specific optical preforms [1-11], and even directly into fibres [12] to enable a vision of desktop optical fibre manufacture accessible to all [5,6], will disrupt traditional fabrication using chemical vapour deposition (CVD) whether on the inside (using modified CVD or MCVD) or on the outside (outside vapour deposition or OVD). Fabrication is potentially customisable in unprecedented ways through choice of 3D printing methods and materials, thermal and optical (fused deposition modelling FDM, direct light projection DLP, stereolithography SLA which relies on a UV laser, selective laser sintering SLS and so on – each has their own advantages and disadvantages which can favour some parameters over others). Complex designs such as structured optical fibres including low loss single-material structured fibres [13,14], metamaterial Fresnel fibres [15,16], photonic crystal fibres [17,18] and antiresonant fibres [19] benefit. Perhaps the biggest impact will be in conventional optical step-index optical fibre fabrication because current commercial CVD processes are constrained by a lathe that spins a tube into which material is sprayed and consolidated in various forms, producing single and centred core preforms from which standard optical fibres are drawn. This constraint does have important advantages. The highly uniform radial symmetry in temperature and pressure during manufacture, gives rise to high structural symmetry critical for low loss scattering and generating degenerate polarisation states within an optical fibre. That also benefits some application specific fibres more than others – for structured optical fibres, for example, high radial preform symmetry permits simple radial analytical relationships describing pressure and uniformity within holes that can be integrated into a drawing process to control their size and wall thicknesses [20]. To fabricate multicore preforms, however, multiple single core preforms are fabricated, the cores etched and then assembled into the desired layout. This is a highly time consuming and laborious process. Given the increasing desire for multi-core fibres playing a role in extending optical bandwidth in communications and data transfer [21], it will not be tolerated longer-term. Consequently, the removal of this centre constraint in preform manufacture is a necessary requirement even though this will be accompanied by other challenges. This is where additive manufacture can come into its own by removing this constraint

altogether – the successful fabrication of multicore, multi dopant active fibres directly from 3D printed preforms demonstrates the comparative simplification of optical fibre manufacture possible [11]. The results suffer from some significant distortion in core shape, a problem that appears unique to additive manufacture in part because it does not involve the spinning of a CVD lathe, the very property that makes multi-core fabrication by traditional means complicated. Although the preform manufacture involved direct light project (DLP) printing and there were some resolution limits in feature shapes and size, the bulk of the core distortion and diffusion was observed after fibre drawing. The induced non-adiabatic asymmetry within otherwise reasonable single mode cores, gives rise to scattering losses accounting for the bulk of the observed losses [4,7]. In all other respects, the fibre production was excellent with scope for future progress and improvement. Promisingly, there is little evidence that additive manufacturing cannot compete with CVD methods if the source of this asymmetry arising during drawing can be identified. In that work, several practical issues arose which forms the subject of this work – the use of various dopants has provided some insight on the nature of the problems arising during preform drawing, offering simple solutions to resolve these matters.

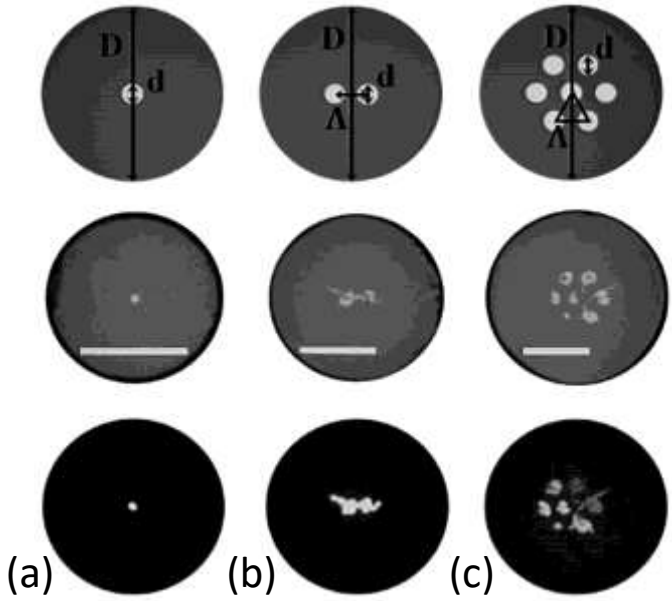

Figure 1. Single (a), dual (b) and seven (c) core fibres are designed (top), fabricated and drawn (middle). The lower image row is for the projected optical light (incoherent white light) transmitted through the fibre. The complex core profiles are illustrated by the 1:1 reproduction of the core profile on the projected far-field image. Image is modified from Figure 1 ref [11].

2. Review of previous results

The previous results [11] on fabricating single and multicore silicate preforms doped with various dopants and then drawing into optical fibre are reproduced in Figures 1 and 2. The intention of the doping in that work was focused on improving gain of rare earth ions combined with Bi moieties [22]. The combination of two species can potentially expand and flatten further the near IR gain spectra to cover all bands. To increase the refractive index, both germanate and titanate was incorporated into the glass matrix. Interestingly, the former is a strong glass softener whilst the latter is a glass hardener – the terms reflect the changes in glass transition of the mixed glass system. Table 1 summarise the properties of the pure oxides of each dopant.

Table 1. Properties of the oxides (derived from various online sources)

	SiO_2 [23]	GeO_2	TiO_2
m.p. (°C)	1600	1115	1843
ρ (g/cm^3)	~2.65	~3.66 [24]	~4.23
α (x 10 $^{-6}$/K)	0.55	7.5 – 8.0 [25,26]	-10.4 [27]
n @1550 nm	~1.45	~1.65	~2.45

3. Fabrication details

These fibres are drawn directly on a modified chemical vapour deposition (MCVD) draw tower from preforms fabricated by additive manufacture. The specific printing approach involves direct light projection (DLP) imaging where the preforms are built upwards using vertically stepped 2D layer by layer through exposure to near UV ($\lambda \sim 385$ nm). The preforms are assembled from a mix of nanoparticles so that a solid capillary tube with a hole for a core is printed first. The bulk of the composition is [SiO_2] ~ 37.4 wt%, a monomer [2-hydroxyethyl methacrylate] ~ 36.9 wt%, monomer solvent [2-phenoxyethanol] ~ 19 wt%, a cross-linker [2-phenoxyethanol] ~ 6.4 wt% and trace amounts of photo-initiator [diphenyl(2,4,6- trimethylbenzoyl) phosphine oxide] ~ 0.2 wt% that polymerise these components are added. An inhibiter ([hydroquinone] ~ 0.1 wt%) is also present to prevent any polymerisation taking place prior to manufacture. The dopant mixture making up the core is similar ([SiO_2] ~ 32.2 wt%, [2-hydroxyethyl methacrylate] ~ 38.6 wt%, [2-phenoxyethanol] ~ 19.9 wt%, [2-phenoxyethanol] ~ 6.7 wt%, [diphenyl(2,4,6- trimethylbenzoyl) phosphine oxide] ~ 0.2 wt%) but with added dopants ([GeO_2] ~ 1.2 wt%, [TiO_2] ~ 0.8 wt%, [$Bi_2(Al_2O_4)_3$] ~ 0.1 wt%, [$ErCl_3$] ~ 0.014 wt % and an added initiator [2,2-azobis(2-methylpropionitrile] ~ 0.25 wt%). Again, with annealing moisture and organic components can be removed, leaving behind the higher temperature materials. The core material was poured into the channels of the printed cladding preform and cured at $T = 60$ and 90 ℃ for times of $t = 2$ and 0.5 hrs, respectively. Various stages of annealing, from 200 to 1200 °C, were carried out ensuring removal of both moisture and organic materials prior to drawing.

The next stage of fibre production is to draw these preforms on a draw tower. In the work reported, the conditions were very close to normal MCVD fibre drawing, made possible by using an outer Heraeus tubing around the 3D printed preform. Although this was not desirable, it was done because the tubing greatly relaxed the handling and placement of the preform in the draw tower. It also elevates the temperature required for drawing, making it comparable to standard MCVD drawing albeit a little lower at $T = 1850$ °C under a drawing pressure of 50 mbar. This is something we shall see has likely played a crucial role in determining the quality of the final fibre. Details of fabrication can be found in the earlier works. Three preforms containing one, two and seven cores were printed and drawn.

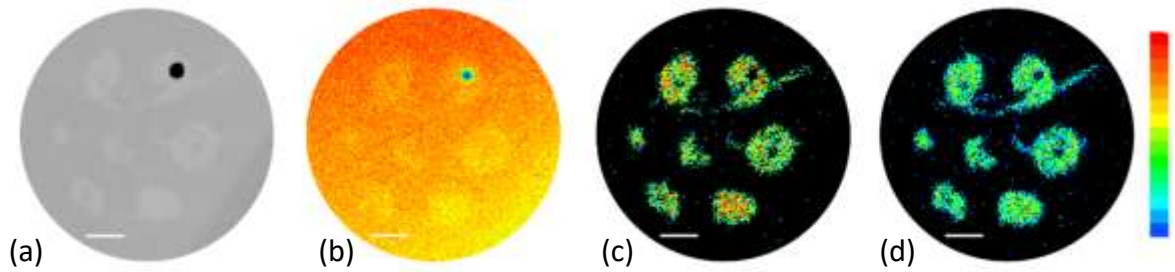

Figure 2. These images show elemental analysis of the seven-core fibre using an electron microprobe and wavelength dispersive analysis of the generated x-rays to identify the elements. (a) shows the SEM image the presence of a surface impurity, either an air channel drawn from a bubble or an aggregation of soot particulate impurity that was unable to diffuse, (b) Si distribution, (c) Ge distribution and (d) Ti distribution. Al, Bi and Er were not profiles as their concentrations were too low to detect clearly. The scale bar is 10 μm. Image is reproduced from Figure 2 ref: [11].

4. Results

Figure 1 shows the fabricated optical fibre core profiles both through optical microscopy images and through optical project of light traveling through the fabricated fibres. Within optical resolution the single core shows relatively good symmetry and a round profile. Adding additional cores deteriorates this profile – in the two-core case, there appears to be diffusion of the core structure into the cladding. This gets significantly worse in the seven-core fibre where the cores diffuse into spiral structures.

A closer examination of the composition of the seven-core fibre through electron microprobe analysis, shown in Figure 2, shows that diffusion of both germanium and titanium oxides has indeed occurred. This can also be observed in the micrograph, consistent with a change in index associated with those glasses, which from Table 1 is expected to increase. Despite substantially different melting points, expansion coefficients and densities (Table 1), they both follow a similar diffusion profile although the titanium oxide has spread further. The measured Si in this region appears to also follow the dopants. There is Si left in the central region after both Ge and Ti have moved away. The separation of the materials may be partially explained by their coordination mismatch and by examining the differences in thermal expansion coefficients – for the amounts of GeO_2 and TiO_2 present, they are close to cancelling their impact on silica. The thermal expansion coefficient is increased adding germanium but decreased adding titanium and for the amounts used in these preforms, the expansion changes are close to offsetting each other. Both will phase separate from the silica because of the bond angle mismatch arising from six coordinate lattice mismatch between GeO_2 and silica and more rigid, denser four-coordinate metallic bonding with TiO_2 (this bonding is responsible for the reduced thermal dependence of expansion and the increased brittleness observed in titanate doped silica fibres).

In the optical image in Figure 2 (a), a strong impurity channel is observed – it correlates with a strong depletion of Si seen in Figure 2 (b), suggesting an air bubble or other immiscible material such as carbon build-up from residue that was not extracted during annealing. This defect is not observed elsewhere in the cross-section although in Figure (c) and (d) both Ge and Ti are depleted from the centre of most of the cores as diffusion occurs.

The diffusion of the dopants as they spread outwards is important – for substantial diffusion of this nature, both the core and cladding must be soft, even liquid, expected at the drawing temperature used (Table 1). All three major constituents melt at the drawing temperature, with GeO_2 more volatile with a higher expansion coefficient driving the tensile stress frozen into the fibres upon cooling. The high expansion coefficient along with liquid behaviour suggests flow so the GeO_2 can initially expand and push outwards but also flow back inwards. Contrastingly, the more viscous TiO_2 despite little expansion is pushed outwards by the GeO_2 even as the latter flows back in. This difference in melting point, density and

expansion coefficient may explain the origin of what appears to be turbulent flow especially if any asymmetry is present – local asymmetry at each core can arise just from the distribution of cores across the fibre. These complex fluid dynamics reflect the local variations arising as a result of having different glassy materials and this will scale with the number of cores present. In the single core case the diffusion is least, in part contained by symmetry and an effective lower melting point since there is less dopant. With two cores, radial variations arise between them and this drives a linear-like diffusion along the core axis. The situation is more complex with seven cores where materials literally spiral around their centre as they diffuse outwards. From a simple superposition assumption, the more cores equate to more material that reduces the amount of silica and therefore creates a greater drop in net melting temperatures relative to the drawing temperatures used. It is interesting to note that beyond a general trend, the superposition principle often used to assess mechanical properties in the solid state offers little additional insight once melting and material separation occurs.

Whilst the complex details of the processes at very high temperature need further investigation, they do highlight a potentially tractable problem with the fabrication method – the drawing temperature is simply too high determined not by the preform composition but by the high temperature silica Heraeus tubing. The silica cladding is made up of silica nanoparticles which generally, through a larger surface area exacerbated by out diffusion of resin materials during fabrication, tend to melt at lower temperatures, closer to $T \sim 1600\ ^{\circ}\mathrm{C}$. The temperature difference with drawing is substantial and leads to a highly softened, if not liquid, internal preform structure that accounts for all the observations made. Further, the effective melting point, and therefore diffusion of the glass system, will increase with more cores because the net dopant material increases. The immediate solution is to replace the Heraeus tubing with a lower temperature glass tube such as borosilicate.

5. Conclusions

Finally, in conclusion a critical assessment of recent work in terms of glassy material properties can explain the origin of complex dynamic behaviour during fabrication. Too high drawing temperature leads to fluid-like flow and evidence of complex vortex formation is observed. This is explained by noting local surrounding variation around each core differ and so stresses and forces also differ. These lead to dopants unevenly spreading outwards and in the multi-core fibres doing so in a spiral manner. Existing asymmetries exacerbate the situation. This problem will apply to all optical fibres with reduced tolerance found with increasing cores as the net percentage of dopants increases and silica decreases. It is not limited to additive manufacture but has featured prominently because conventional manufacturing uses the Heraeus tubing as the cladding and does not have the porous structure arising from printing. As the number of cores increases, the drawing temperature must be adjusted accordingly depending on the number, the compositions and the tolerances in drawing. Surrounding asymmetry can further complicate this – this may be the shape of the preform, the position of the cores or simply the method of drawing. In the work analysed here, an outer higher temperature silica tube was used to fix the 3D printed preform and simplify mounting. However, this has led to constraints and the need for higher drawing temperatures relative to the melting point of the core materials. This can be overcome by replacing the tube with a lower melting point glass and reducing the drawing temperature. Alternatively, the use of a supporting tube can be avoided. Critical analysis has identified common drawing problems that can be avoided irrespective of the preform manufacturing process – there is little reason why optical fibre produced by additive manufacture cannot eventually compete with conventional manufacturing.

References

[1] Cook K, Canning J, Leon-Saval S, Redi Z, Hossain M A, Comatti J E, Luo Y, Peng G-D 2015 Air-structured optical fibre drawn from a 3D-printed optical preform *Opt. Lett.* **40** (17) 3966 – 3999

[2] Cook K, Balle G, Canning J, Chartier L, Athanze T, Hossain M A, Han C, Comatti J E, Luo Y, Peng G-D 2016 Step-index optical fibre drawn from 3D printed preforms *Opt. Lett*. **41** (19) 4554 - 4557
[3] Toal P M, Holmes L J, Rodriguez R, Wetzel E D 2017 Microstructured monoflament via thermal drawing of additively manufactured preforms *Addit Manuf.* **16** 12 – 23
[4] Chu Y, Fu X, Luo Y, Canning J, Tian Y, Cook K, Zhang J, Peng G-D 2019 Silica optical fibre drawn from 3D printed preforms *Opt. Lett.* **44** (21) 5358 – 5361
[5] Canning J 2019 3D Printing and Optical Waveguide Technologies *10th Int. Conf. Mater. for Adv. Technologies (ICMAT 2019)* Singapore, Invited
[6] Canning J 2020 3D Printing and Photonics *4th Int. Conf. Emerging Adv. Nanomat. (ICEAN)* Newcastle University Australia, Keynote
]7] Luo Y, Canning J, Zhang J, Peng G-D 2020 Towards optical fibre fabrication using 3D printing technology *Opt. Fibre Tech*. **58**, 102299
[8] Rosales A L C, Velázquez M M A N, Zhao X, Sahu J K 2020 Optical fibres fabricated from 3D printed silica preforms, *Proc. SPIE 11271, Laser 3D Manufacturing VII,* SPIE; paper 112710U
[9] Canning J, 2021 3D printing optical preforms and fibres *12th Int. Conf. on Information Optics & Photonics (CIOP),* Xian China, Invited
[10] van der Elst L, de Lima C F, Kurtoglu M G, Koraganji V N, Zheng M, Gumennik A 2021 3D Printing in Fiber-Device Technology. *Adv. Fiber Mater*. **3** 59 – 75
[11] Chu Y, Fu X, Luo Y, Canning J, Wang J, Cook K, Ren J, Zhang J, Peng G-D 2021 Additive Manufacturing Structured Silica Optical Fibers with Functional Dopants, *Light: Advanced Manufacturing*
[12] Canning J, Hossain M A, Han C, Chartier L, Cook K, Athanaze T 2016 Drawing optical fibres from three-dimensional printers *Opt. Lett*. **41**(23) 5551 – 5554
[13] Kaiser P V, Astle H W 1974 Low-loss single material fibers made from pure fused silica *Bell Syst. Tech. J*. **53** (6) 1021 – 1039
[14] Knight J C, Birks T A, Russell P S J, Atkin D M 1996 Pure silica single mode fibre with hexagonal photonic crystal cladding *Conf. Optical Fiber Commun. (OFC),* San Jose, CA, Paper PD3.
[15] Canning J, Buckley E, Lyytikainen K, 2003 Multiple Source Generation using Air-Structured Optical Waveguides for Optical Field Shaping and Transformation Within and Beyond the Waveguide *Opt. Express* **11** (4) 347 – 358
[16] Martelli C, Canning J 2007 Fresnel fibres with omni-directional zone cross-sections, *Opt. Express* **15** (7) 4281 – 4286
[17] Russell P S J 2003 Photonic crystal fibers *Science* **299** (5605) 358 – 362
[18] Bjarklev A, Broeng J, Bjarklev A S, 2003 *Photonic Crystal Fibres* (USA: Springer-Verlag New York Inc)
[19] Sakr H, Chen Y, Jasion G T, Bradley T D, Hayes J R, Mulvad H C H, Davidson I A, Fokoua E N, Poletti F, 2020 Hollow core optical fibres with comparable attenuation to silica fibres between 600 and 1100 nm *Nat. Commun.* **11** 6030
[20] Tafti G, Canning J, Wang S, Luo Y, Cook K, Peng G-D 2021 Pressure Effects on Structured Optical Fibre Drawing by Modified Single-Capillary Modelling, *Opt. Fibre Tech.*, **63** 102528
[21] Jung Y, Alam S, Richardson D J, Ramachandran S, Abedin K S 2020 Multicore and multimode optical amplifiers for space division multiplexing, in *Optical Fiber Telecommunications VII* (Academic Press) chapter 7 p. 301
[22] Zhao Q, Luo Y, Wang W, Canning J, Peng G-D 2017 Enhanced broadband near-IR luminescence and gain spectra of bismuth/erbium co-doped fiber by 830 and 980 nm dual pumping, *AIP Advances* **7** 045012
[23] Properties of Silicon Dioxide https://www.azom.com/properties.aspx?ArticleID=1114
[24] Kamiya K. Yoko T, Itoh Y, Sakka S 1986 X-ray diffraction study of $Na_2O - GeO_2$ melts *J. Non-Crystal. Solids* **79** 285 – 294
[25] Huang Y Y, Sarkar A, Schultz P C 1978 *J. Non-Crystal Solids* **27** 29
[26] Birtch E M, Shelby J E 2006 *Phys. Chem. Glasses* **47** 182
[27] Kamiya K, Sakka S 1982 Thermal expansion coefficient of TiO_2-SiO_2 and TiO_2-GeO_2 glasses *J. Non-Crystal. Solids* **52** 357 - 363

Acknowledgments
Private funding supporting this work is acknowledged.